





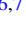






First Results of an ALMA Band 10 Spectral Line Survey of NGC 6334I: Detections of Glycolaldehyde (HC(O)CH₂OH) and a New Compact Bipolar Outflow in HDO and CS

Brett A. McGuire^{1,2,10} , Crystal L. Brogan¹ , Todd R. Hunter¹ , Anthony J. Remijan¹ , Geoffrey A. Blake^{3,4} ,
Andrew M. Burkhardt^{5,11} , P. Brandon Carroll², Ewine F. van Dishoeck^{6,7} , Robin T. Garrod^{5,8} , Harold Linnartz⁹ ,

Christopher N. Shingledecker^{8,12} , and Eric R. Willis⁸ 

¹ National Radio Astronomy Observatory, Charlottesville, VA 22903, USA; bmcguire@nrao.edu

² Harvard-Smithsonian Center for Astrophysics, Cambridge, MA 02138, USA

³ Division of Geological and Planetary Sciences, California Institute of Technology, Pasadena, CA 91125, USA

⁴ Division of Chemistry and Chemical Engineering, California Institute of Technology, Pasadena, CA 91125, USA

⁵ Department of Astronomy, University of Virginia, Charlottesville, VA 22904, USA

⁶ Leiden Observatory, Leiden University, 2300 RA Leiden, The Netherlands

⁷ Max-Planck Institut für Extraterrestrische Physik, Giessenbachstr. 1, D-85748 Garching, Germany

⁸ Department of Chemistry, University of Virginia, Charlottesville, VA 22904, USA

⁹ Sackler Laboratory for Astrophysics, Leiden Observatory, Leiden University, 2300 RA Leiden, The Netherlands

Received 2018 July 2; revised 2018 August 1; accepted 2018 August 2; published 2018 August 17

Abstract

We present the first results of a pilot program to conduct an Atacama Large Millimeter Array (ALMA) band 10 spectral line survey of the high-mass star-forming region NGC 6334I. The observations were taken in exceptional weather conditions (0.19 mm precipitable water) with typical system temperatures $T_{\text{sys}} < 950$ K at ~ 890 GHz. A bright, bipolar north–south outflow is seen in HDO and CS emission, driven by the embedded massive protostar MM1B. This has allowed, for the first time, a direct comparison of the thermal water in this outflow to the location of water maser emission from prior 22 GHz Very Large Array observations. The maser locations are shown to correspond to the sites along the outflow cavity walls, where high-velocity gas impacts the surrounding material. We also compare our new observations to prior *Herschel* Heterodyne Instrument for the Far-infrared (HIFI) spectral line survey data of this field, detecting an order of magnitude more spectral lines (695 versus 65) in the Atacama Large Millimeter/submillimeter Array (ALMA) data. We focus on the strong detections of the complex organic molecule glycolaldehyde (HC(O)CH₂OH) in the ALMA data that is not detected in the heavily beam-diluted HIFI spectra. Finally, we stress the need for dedicated THz laboratory spectroscopy to support and exploit future high-frequency molecular line observations with ALMA.

Key words: astrochemistry – ISM: individual objects (NGC 6334I) – ISM: jets and outflows – ISM: molecules – masers

1. Introduction

Observations with the Atacama Large Millimeter/submillimeter Array (ALMA) in bands 3–7 (84–373 GHz) have proven to be exceptional tools for the detection of new molecular species in the interstellar medium (ISM) and the study of their chemical history and interaction with their physical environment. As a few examples, Belloche et al. (2014) reported the first detection of a branched carbon-chain molecule in the ISM, isopropyl cyanide (C₃H₇CN), in band 3 observations of Sgr B2. Later, McGuire et al. (2017) detected methoxymethanol (CH₃OCH₂OH) in surprisingly high abundance toward NGC 6334I in bands 6 and 7 observations, while Fayolle et al. (2017) identified methyl chloride (CH₃Cl) for the first time using band 7 observations of IRAS 16293-2422. These observations, among many others, demonstrate the power of ALMA for studies of our molecular universe in the 1–3 mm wavelength range.

Astrochemical observations at higher frequencies, in ALMA bands 9 (602–720 GHz) and 10 (787–950 GHz) offer complementary benefits to the lower-frequency data, yet few molecular line surveys have been conducted at these frequencies. Here, we explore two advantages of high-frequency spectral line observations. First, the fundamental or first few lowest transitions of many small molecules of interest fall into this range. For example, the HDO $1_{1,1}-0_{0,0}$ fundamental transition occurs at 893.6 GHz (Messer & De Lucia 1984), providing one of the best opportunities to obtain ground-based measurements of thermal water (see, e.g., Comito et al. 2003).

Second, the transitions of most complex organic molecules (COMs) that fall within this frequency range are typically much higher in energy, providing a robust constraint on excitation conditions within a source. For example, the strongest transitions of glycolaldehyde (HC(O)CH₂OH), the simplest sugar-related molecule, in band 6 have upper-state energies $E_u \sim 60$ –200 K in the ground vibrational state. As a result, analysis of the emission of this molecule can be biased toward lower-excitation conditions, although this can be mitigated through the observation of vibrationally excited states in some cases (Jørgensen et al. 2012). Complementary observations at higher frequencies, however, provide access to higher-energy lines to rigorously constrain these excitation temperatures—the strongest transitions of HC(O)CH₂OH in band 10 have $E_u = 530$ –630 K—and can provide needed confirmatory

¹⁰ B.A.M. is a Hubble Fellow of the National Radio Astronomy Observatory.

¹¹ Current Address: Submillimeter Array (SMA) Postdoctoral Fellow, Harvard-Smithsonian Center for Astrophysics, Cambridge, MA 02138.

¹² Current Address: Alexander von Humboldt Foundation Postdoctoral Research Fellow, Max Planck Institute for Extraterrestrial Physics, Garching, Germany; Institute for Theoretical Chemistry, University of Stuttgart, Stuttgart, Germany.

transitions to secure a lower-frequency detection (see, e.g., Jørgensen et al. 2012).

These higher-energy transitions also provide selective access to the warmest molecular gas in a source, which prior studies have shown can have substantially different chemistry from the population probed by the lower-energy transitions accessible at lower frequencies (Crockett et al. 2014). There is, however, a relative lack of direct laboratory measurements of molecular spectra above ~ 600 GHz, meaning that many identifications are made from extrapolated quantum mechanical fits. For some species this is a reasonably accurate process, but, as will be shown later, the richness of the band 10 spectra underscores the need for dedicated high-frequency laboratory work. Finally, at these frequencies it is reasonable to expect that increased dust optical depth effects might “hide” the deepest, most compact regions of hot molecular cores, and the bright continuum might drive many molecular transitions into absorption.

To explore the utility of ALMA band 9/10 observations, we proposed for a full band 9 survey, and a pilot band 10 survey, of the high-mass star-forming region NGC 6334I in Cycle 5. NGC 6334I was chosen as the target for three reasons. First, it is an exceptionally molecular line-rich source (McGuire et al. 2017) with a relatively small heliocentric distance of 1.3 kpc (Chibueze et al. 2014; Reid et al. 2014). Second, it has previously been targeted by single-dish observations in overlapping frequency ranges by Zernickel et al. (2012) using the Heterodyne Instrument for the Far-Infrared (HIFI; de Graauw et al. 2010) on the *Herschel Space Observatory* (Pilbratt et al. 2010). Third, it displays a complex spatial structure consisting of a substantial number of embedded sources and outflows, and several chemically distinct regions separated by only ~ 2000 au ($\sim 1''5$; Brogan et al. 2016; McGuire et al. 2017; Bøgelund et al. 2018; Figure 1).

Here, we present a first look at ALMA band 10 observations of any line-rich source, and discuss the results in the context of both probing favorable transitions of light molecules, and in examining the high-excitation lines of complex organic species. The spectra at these high frequencies are as line-rich as those in the millimeter regime. Contrary to initial expectations, observations of high-mass star-forming regions like NGC 6334I at ALMA band 10 do not appear to be substantially hampered by dust opacity, and are in fact generally better suited than previous single-dish facilities such as *Herschel*. These first-look observations demonstrate the power and versatility of high-frequency observations with ALMA.

2. Observations and Data Reduction

The band 10 observation occurred 2018 April 05, with 40 ALMA antennas in the array in a nominal C43-3 configuration with a maximum baseline of 532 m providing a $0''.21 \times 0''.15$ synthesized beam (robust weighting parameter = 0.5). The precipitable water vapor at the time of observation was 0.19 mm, and the average resulting system temperature was $T_{\text{sys}} = 926$ K at 880 GHz. Total time on source was 47 minutes, resulting in an rms noise level of 62 mJy beam $^{-1}$ in 0.5 km s $^{-1}$ channels. J1517-2422 (~ 1.85 Jy at 880 GHz) was used as the flux and bandpass calibration source; J1733-3722 (~ 0.43 Jy at 880 GHz) was the phase calibrator.

At 880 GHz, the half power primary beam width is $\sim 6''.6$, which is slightly smaller than the total angular extent of the emitting regions of interest in NGC 6334I. We therefore targeted two phase centers to cover the entire source while maximizing the ultraviolet (UV) coverage and rms sensitivity

in the critical central regions. At the time of publication, only the pointing position toward MM1 has been observed; with a phase center of $\alpha(\text{J2000}) = 17^{\text{h}}20^{\text{m}}53^{\text{s}}.3\delta$ (J2000) = $-35^{\circ}46'59''.0$ (Figure 1). The 0.35 mm continuum was created from (relatively) line-free channels, and has an aggregate bandwidth and rms noise of 2.7 GHz and 50 mJy beam $^{-1}$, respectively. The method employed for continuum subtraction is described in detail in Brogan et al. (2018). Self-calibration was performed on the continuum and applied to the spectral line data after subtracting the continuum in the UV plane. The details of the complementary band 7 data used in this Letter are described in McGuire et al. (2017), while the band 4 data are described in the Appendix.

For the analysis presented here, spectra were extracted toward MM1 from a single pixel at a position of $\alpha(\text{J2000}) = 17^{\text{h}}20^{\text{m}}53^{\text{s}}.374\delta$ (J2000) = $-35^{\circ}46'58''.34$ (magenta cross in Figure 1). The location is ~ 400 au west of the brightest continuum peak, MM1B. This location was chosen for its proximity to the dense molecular gas while being far enough from the bright continuum that the majority of the molecular lines are not driven into absorption due to the high continuum brightness temperature (McGuire et al. 2017).

The NGC 6334I region was previously targeted in an extensive broadband spectral line survey as part of the Chemical *Herschel* Surveys of Star-forming regions (CHESS; Ceccarelli et al. 2010) key program using HIFI (Zernickel et al. 2012). The data used in this manuscript for comparison to our ALMA data were obtained from the *Herschel* Science Archive, ObsID 1342192328. The HIFI data are used directly as downloaded from the archive, with the exception of the subtraction of a static continuum offset, to place the spectral baseline at $T_A = 0$ K.

3. HDO and CS

Most transitions of H₂O are blocked from the ground by atmospheric absorption features, and thus observations normally rely either on extreme excitation conditions (i.e., maser emission), isotopologues, or space-based observatories to study H₂O. Spectra toward NGC 6334I, Orion KL, and other star-forming regions in the rotational and lowest few ground-state transitions of ortho-H₂O recorded by the *Submillimeter Wave Astronomy Satellite* (SWAS) and *Herschel* exhibit broad wing components that arise from heated gas in low- and high-velocity outflowing gas (Melnick et al. 2000; Neufeld et al. 2000; van der Tak et al. 2013; San José-García et al. 2015). Our band 10 observations provide access to the HDO fundamental $1_{1,1}-0_{0,0}$ transition at 893.6 GHz ($E_u = 43$ K) and the higher-energy ($E_u = 581$ K) $6_{2,4}-5_{3,3}$ transition at 895.9 GHz (Messer & De Lucia 1984).

Figure 1 shows the full velocity extent of these HDO transitions as both peak intensity and integrated intensity images. While no emission signals of this transition were detected in the HIFI data (Emprechtinger et al. 2013), the lower-energy, fundamental HDO transition shows an extended distribution in the high-resolution ALMA data. The higher-energy transition is more compact and located closer to the primary continuum sources, likely tracing warmer regions within the source. This pattern is similar to that measured in Orion KL for two intermediate energy transitions in ALMA band 6 (Neill et al. 2013). It is notable that the fundamental transition of HDO exhibits significant self-absorption toward the bright continuum sources, and even the $6_{2,4} - 5_{3,3}$ transition is

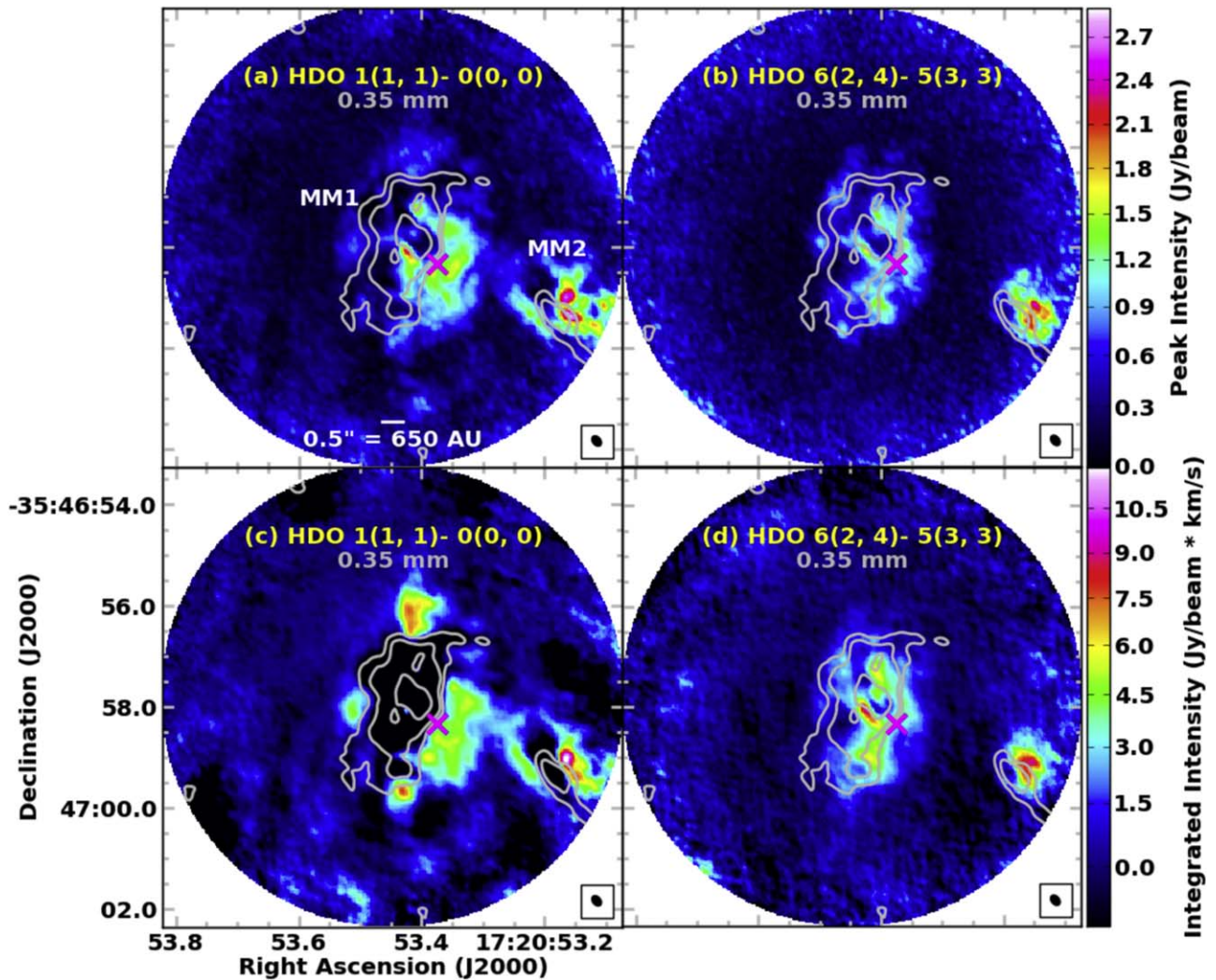


Figure 1. ALMA band 10 images of the peak (a, b) and integrated intensity (c, d) from -13.5 to $+2.5$ km s^{-1} for two transitions of HDO with 0.35 mm dust continuum contours overlaid. The 0.35 mm dust continuum contour levels are 50, 75, and 150 K on the Planck temperature scale. Magenta \times symbols show the location of the spectra extracted for MM1 (Figure 3). There is substantial absorption of the ground-state transition of HDO toward the MM1 continuum in the integrated intensity maps. This absorption dominates the integrated intensity map, leaving no net emission signal, whereas the peak intensity maps show the locations of this subsumed HDO emission. Primary beam correction has been applied with a cutoff at 0.25 of the FWHM. The synthesized beam of $0''.23 \times 0''.16$ (PA = 39°) is shown in the lower right of each panel.

affected by the high continuum opacity and brightness temperature at the continuum peak locations (see Figure 1).

Figure 2(a) shows only the redshifted, high-velocity components of the HDO emission, and reveals a structure that traces a north–south bipolar outflow emanating out of the MM1 continuum peak, centered on the MM1B protostellar source. Our data also covered the CS $J = 18-17$ transition ($E_u = 402$ K) at 880.9 GHz (Müller et al. 2005), which shows the same north–south outflow structure as HDO (Figure 2(b)). This outflow, called the MM1B N-S outflow, has also been detected in ALMA CS (6–5) emission by Brogan et al. (2018). These authors find a total linear extent of $6''.2$ (8060 au) for MM1B N-S, and that its orientation is nearly in the plane of the sky, leading to a very young dynamical time of only 166 years.

Extensive observations of H₂O masers have been made toward NGC 6334I at cm-wavelengths both with single-dish monitoring (MacLeod et al. 2018) and recent complementary Karl G. Jansky Very Large Array (VLA) interferometric

observations (Brogan et al. 2016, 2018). By overlaying the locations of cm-wavelength H₂O masers from the VLA data, it becomes apparent that the masers are predominantly tracing the walls of this outflow cavity where the high-velocity gas likely impacts the surrounding quiescent gas. These locations are consistent with water maser pumping models in which the observed masers arise from velocity-coherent structures in the hot gas behind shocks propagating in dense regions (Melnick et al. 1993; Hollenbach et al. 2013). The ability to monitor both the thermal water in the outflow and pinpoint the locations of the H₂O maser emission to the impact sites of the outflow into the surrounding media demonstrates the powerful combination of ALMA band 10 data with VLA cm-wave observations. In this case, the detection of a collimated outflow in thermal and maser lines along the same axis as the compact radio jet from MM1B (Brogan et al. 2018; Hunter et al. 2018) enables the recognition of these various distinct phenomena as arising from a unified structure.

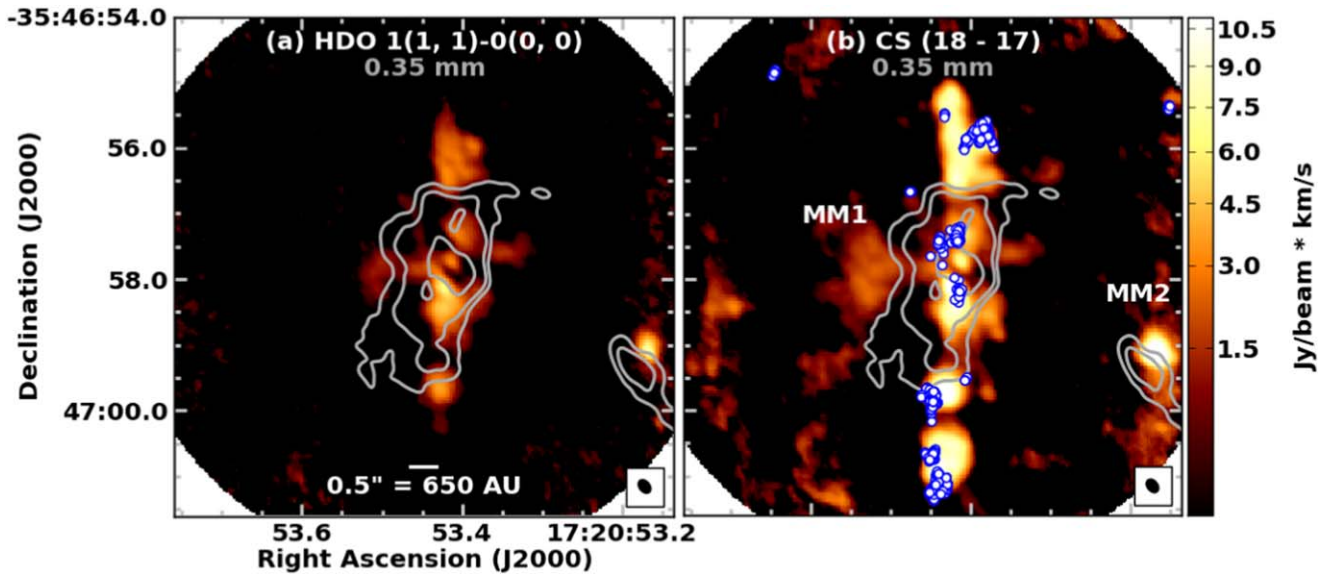


Figure 2. ALMA band 10 images of the integrated intensity of the redshifted high-velocity gas (-3 to $+2.5$ km s^{-1} ; the systemic velocity is -7 km s^{-1}) for the (a) ground state of HDO and the (b) CS (18–17) transition showing a highly collimated north–south outflow emanating from MM1. Blueshifted high-velocity emission (not shown) is co-spatial with the redshifted emission, but is much weaker. The 0.35 mm continuum is the same as Figure 1. White circles show the locations of H_2O masers detected with the VLA in epoch 2017.8 (Brogan et al. 2018). Primary beam correction has been applied with a cutoff at 0.25 of the FWHM. The synthesized beam of $0''.23 \times 0''.16$ ($\text{PA} = 39^\circ$) is shown in the lower right of each panel.

3.1. Spectral Line Survey and Glycolaldehyde ($\text{HC(O)CH}_2\text{OH}$)

The benefits of performing high-frequency spectral line surveys were recognized and exploited by a number of key projects performed with the HIFI instrument aboard *Herschel*. As mentioned earlier, many small molecules have their first few rotational transitions at these higher frequencies, and surveys with HIFI resulted in the first reported detections of SH^+ (Benz et al. 2010), HCl^+ (De Luca et al. 2012), H_2O^+ (Ossenkopf et al. 2010), and H_2Cl^+ (Lis et al. 2010). Additionally, full spectral line surveys provided robust constraints on the excitation conditions and populations of larger molecules (>5 atoms) in a variety of extraordinary molecular sources such as Sgr B2(N) (Neill et al. 2014) and Orion KL (Crockett et al. 2014).

A number of spectral line surveys have been carried out toward NGC 6334I, primarily between 80 and 270 GHz and by *Herschel* HIFI from 500 to 1900 GHz (see Zernickel et al. 2012 and references therein). While these surveys revealed a line-rich source with a complex molecular inventory, the large beam sizes were unable to resolve the underlying structure, and suffered significantly from beam dilution. The overall angular extent of NGC 6334I is $\sim 10'' \times 8''$ ($13,000 \times 10,000$ au), with most complex molecules emitting over an extent of $\leq 5''$ (6500 au; McGuire et al. 2017). In a *Herschel* beam of $\sim 25''$ at 880 GHz, this mismatch results in a factor of $\gtrsim 25$ loss in line brightness due to beam dilution.

Indeed, when compared to the spectral line survey from HIFI presented in Zernickel et al. (2012), the most striking feature of our ALMA band 10 spectra is the greatly enhanced line density, and the number of lines that are optically thick. Figure 3 shows the full ~ 8 GHz spectral coverage in the lower sideband of the ALMA data toward MM1 compared with the HIFI data at the same frequency. The line density in the ALMA spectrum is ~ 10 times that of HIFI (695 versus 65 lines in the ALMA versus HIFI spectra over the same range). This is

exemplified by the emission lines of CH_3OH ($\nu_t = 1$) and C^{18}O seen in each spectrum. The complex molecular emission is significantly enhanced in the ALMA spectra due to its more spatially compact distribution. C^{18}O , conversely, is not optically thick in the ALMA data, with a substantially decreased intensity relative to the complex molecules. This effect is almost certainly due to a more extended distribution that is being partially resolved out in the ALMA observations, but for which the HIFI observations were well suited.

Because the band 10 data are so molecular line-rich, they can provide valuable constraints on molecular excitation and column density derivations if they can be robustly analyzed alongside lower-frequency observations. To test this, we extracted spectra toward the MM1 spectral analysis position from data obtained in previous ALMA observations toward NGC 6334I in band 4 (ADS/JAO.ALMA#2017.1.00661.S) and band 7 (ADS/JAO.ALMA#2015.A.00022.T) and in these band 10 data, all convolved to the smallest common synthesized beam size of $0''.26 \times 0''.26$. A full molecular analysis of the band 10 survey is beyond the scope of this Letter. Once the full band 9/10 spectral survey is complete, we plan to provide a fully reduced line survey to the community. A preliminary inventory of molecules, however, includes ^{13}CO , C^{18}O , H_2CO , HNCO , CH_3OH , $^{13}\text{CH}_3\text{OH}$, $\text{CH}_3^{18}\text{OH}$, $\text{CH}_3\text{OH } \nu_t = 1$, CH_3CN , CH_2NH , CH_3NH_2 , NH_2CHO , $\text{CH}_3\text{CH}_2\text{OH}$, $\text{HC(O)CH}_2\text{OH}$, and CH_3OCHO .

Here, we focus only on $\text{HC(O)CH}_2\text{OH}$, the simplest sugar-related molecule. This COM was successfully detected by ALMA toward the solar-mass protostar IRAS 16293-2422 by Jørgensen et al. (2012), but has not been reported in the HIFI data at band 10 frequencies.

While collisional cross-sections for molecules more complex than methanol (CH_3OH) are generally not available, especially at these frequencies, the high densities in the region (source averaged $n_{\text{H}} > 10^6 \text{ cm}^{-3}$; Russeil et al. 2010) suggest that molecules should be well described by a single T_{ex} . We

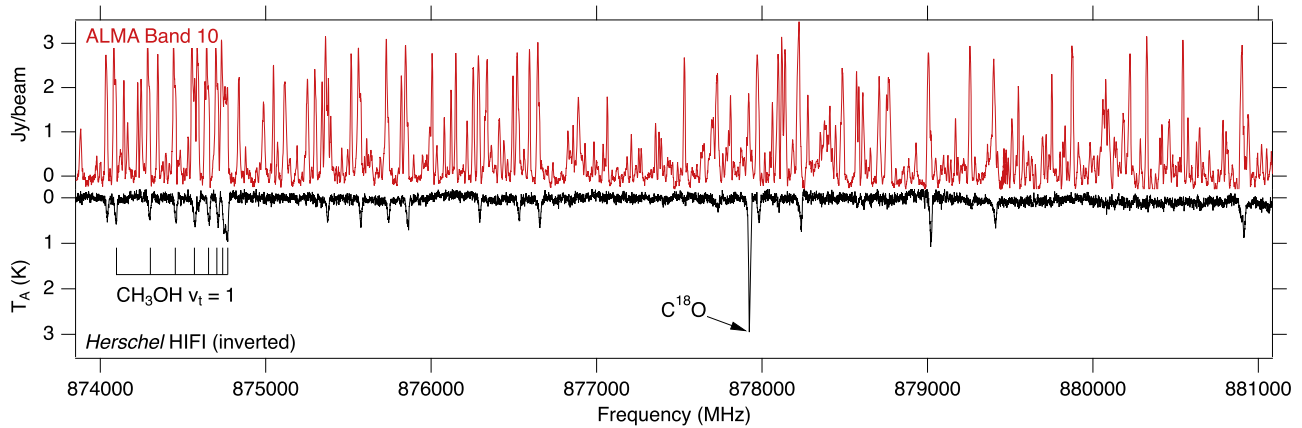


Figure 3. Comparison of this ALMA band 10 data set (top; extracted toward MM1) to observations retrieved from the *Herschel* archive and taken as part of the CHES key program using the HIFI instrument covering the same data range (bottom; Zernicke et al. 2012). The *Herschel* beam ($\sim 25''$ at 880 GHz) covered the entirety of the NGC 6334I region. Note that the ALMA spectra are in Jy/beam, while the *Herschel* data are in antenna temperature, and that the *Herschel* spectra have been inverted for comparison. A constant offset has been subtracted from the *Herschel* data to remove the continuum for presentation purposes. Transitions of $\text{CH}_3\text{OH } v_t = 1$ and C^{18}O are labeled.

therefore used the formalism described in Turner (1991) to simulate the spectrum of $\text{HC(O)CH}_2\text{OH}$ across the entire ~ 750 GHz span in observational coverage, accounting for differences in background continuum temperature at each frequency. The simulated spectra were converted to Jy/beam from Kelvin using the Planck scale, as the Rayleigh–Jeans approximation introduces significant errors at band 10 frequencies. The simulated $\text{HC(O)CH}_2\text{OH}$ spectra are enabled by the high-frequency laboratory work of Carroll et al. (2010) that extended the measured frequencies from 354 GHz to 1.2 THz.

Figure 4 shows the resulting simulated $\text{HC(O)CH}_2\text{OH}$ emission overlaid on the observational data in bands 4, 7, and 10. We find that assuming a single excitation temperature ($T_{\text{ex}} = 135$ K), linewidth ($\Delta V = 3.2$ km s^{-1}), and column density ($N_T = 1.3 \times 10^{17}$ cm $^{-2}$) across the bands well reproduces the observed emission to zeroth order. The band 10 data provide a high-energy anchor to the excitation conditions; the six lines shown in Figure 4 have upper-state energies between $E_u = 530$ –631 K, compared to $E_u = 63$ –171 K for the band 4 lines shown. A full fit of the spectrum, including line contamination and blending from other species, is beyond the scope of this first-look Letter. Preliminary work indicates the availability of these high- and low-energy anchors provides definite constraints on the excitation temperature of glycolaldehyde to be ~ 135 K.

The peak and integrated intensities of the $\text{HC(O)CH}_2\text{OH}$ transition at 892.12 GHz ($J_{K_a, K_c} = 28_{23, x} - 27_{22, x}$; $E_u = 546$ K) is shown in Figure 5. Toward the MM1 cluster, these high-energy transitions seem to trace a similar, although not identical, distribution to the high-energy HDO lines shown in Figure 1, but has a markedly different distribution toward MM2. Recent laboratory studies have shown that $\text{HC(O)CH}_2\text{OH}$ is readily formed on icy dust grains through hydrogenation of solid CO (Fedoseev et al. 2015). The observed distribution may indicate that after being formed in the ice, some of this condense-phased $\text{HC(O)CH}_2\text{OH}$ is being driven into the gas phase by a non-thermal desorption mechanism such as shock-induced sputtering, as previously hypothesized in observations of complex molecules in galactic center regions (Requena-Torres et al. 2006). Thermal

desorption mechanisms are likely also relevant in many warmer regions of the source.

The richness of the band 10 spectra underscores a need for accurate, high-resolution gas phase spectra of complex molecules from laboratory studies in these frequency ranges. While laboratory data in the millimeter-wave range below ~ 500 GHz are increasingly common, the technical difficulties in measuring and analyzing submillimeter and THz spectra, combined with a general lack of observational applications, has limited the number of groups working in this regime. While a dedicated effort was undertaken to provide $\text{HC(O)CH}_2\text{OH}$ spectra through 1.2 THz, laboratory spectra for many other complex molecules are missing, and transitions in this range must be extrapolated from lower frequencies, leading to increasingly large uncertainties.

4. Conclusions

We have presented a first look at ALMA band 10 spectral line survey toward a line-rich source—the high-mass star-forming region NGC 6334I—obtained in exceptional weather conditions. The resulting map shows a bright, bipolar north–south outflow from the central massive protostar MM1b as traced by both HDO and CS emission. A comparison to archival *Herschel* HIFI data of the source shows the power of spatially resolving underlying substructure with a beam size that is well matched to the source, resulting in the unambiguous identification of $\text{CH(O)CH}_2\text{OH}$. A wealth of additional transitions suggest the presence of additional complex molecules that can be identified once high-resolution laboratory data are available.

The authors thank the anonymous referee for a careful evaluation that improved the quality of this manuscript. This Letter makes use of the following ALMA data: ADS/JAO.ALMA#2017.1.00717.S, #2017.1.00661.S, and #2015.A.00022.T. ALMA is a partnership of ESO (representing its member states), NSF (USA) and NINS (Japan), together with NRC (Canada) and NSC and ASIAA (Taiwan) and KASI (Republic of Korea), in cooperation with the Republic of Chile. The Joint ALMA Observatory is operated by ESO, AUI/

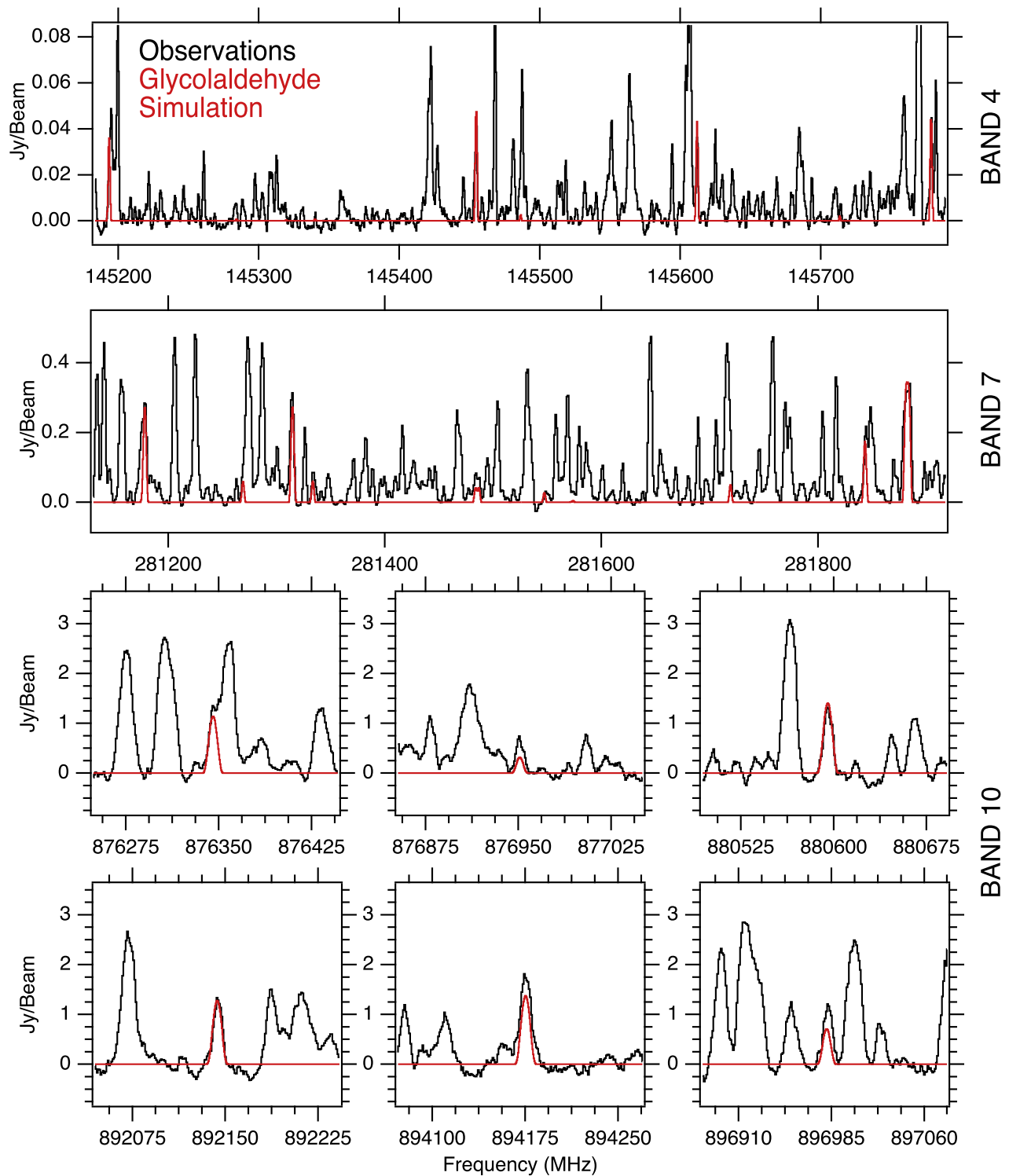


Figure 4. Simulated spectra of $\text{HC(O)CH}_2\text{OH}$ plotted in red over ALMA observations of NGC 6334I MM1 plotted in black. The simulated spectra assume $T_{\text{ex}} = 135$ K, $\Delta V = 3.2$ km s $^{-1}$, and $N_T = 1.3 \times 10^{17}$ cm $^{-2}$, with a $v_{\text{LSR}} = -7$ km s $^{-1}$. The ALMA observations have been convolved to a uniform synthesized beam of $0''.26 \times 0''.26$. In the lower six panels, smaller regions of the frequency coverage in band 10 have been selected to show detail.

NRAO and NAOJ. The National Radio Astronomy Observatory is a facility of the National Science Foundation operated under cooperative agreement by Associated Universities, Inc.

Support for B.A.M. was provided by NASA through Hubble Fellowship grant #HST-HF2-51396 awarded by the Space Telescope Science Institute, which is operated by the

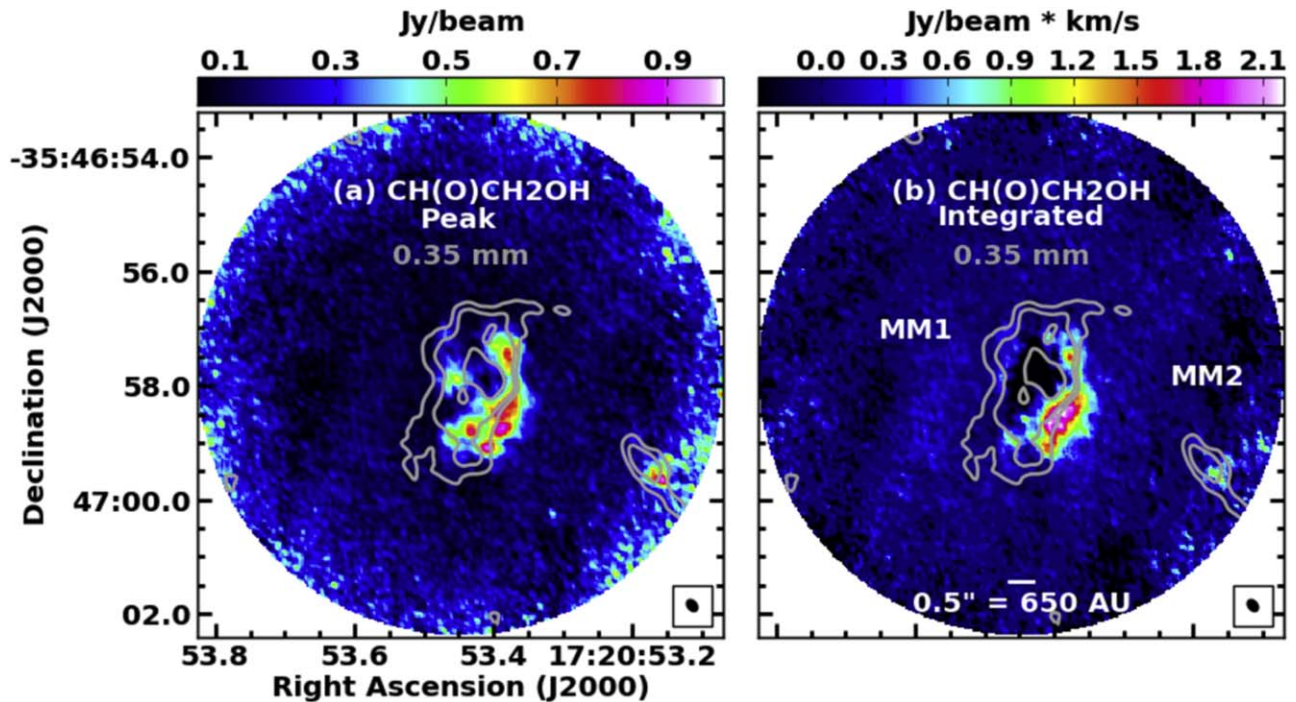


Figure 5. ALMA band 10 images of the peak (a) and integrated intensity (b) of the $\text{HC(O)CH}_2\text{OH}$ transition at 892.12 GHz (28,23–27,22; $E_u = 546$ K) shown in Figure 4. The 0.35 mm continuum is the same as Figure 1 and the synthesized beam is shown in the lower-right corner.

Association of Universities for Research in Astronomy, Inc., for NASA, under contract NAS5-26555. Support for A.M.B. was provided by the NSF through the Grote Reber Fellowship Program administered by Associated Universities, Inc./National Radio Astronomy Observatory and the Virginia Space Grant Consortium. This research made use of NASA's Astrophysics Data System Bibliographic Services, Astropy, a community-developed core Python package for Astronomy (Astropy Collaboration et al. 2013), and APLpy, an open-source plotting package for Python hosted at <http://aplpy.github.com>.






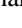





Appendix Band 4 Observations

The salient parameters for the cycle 5 band 4 observations are given in Table 1 and will be discussed in detail in a forthcoming paper by Brogan et al.

Table 1
Observing Parameters for Band 4 ALMA Data

Parameter	Band 4 (2.1 mm)
Project code	ALMA 2017.1.00661.S
Observation date(s)	2017 Dec 3, 7; 2018, Jan 4
Configuration	C43-6
Time on source (minutes)	170
FWHM primary beam	0'69
Polarization products	dual linear
Gain calibrator	J1713-3418
Bandpass calibrator	J1617-5848
Flux calibrator	J1617-5848
Spectral window center freqs. (GHz)	130.5, 131.5, 144.5, 145.4
Spectral window bandwidth (MHz)	4×937.5
Spectral resolution (km s^{-1})	1.1 km s^{-1}
Robust parameter	0.5
Ang. res. ($'' \times ''$ (P.A. $^\circ$))	0.23×0.16 (-86.7)
rms noise per channel ($\text{mJy beam}^{-1} * \text{km s}^{-1}$)	0.8

ORCID iDs

Brett A. McGuire  <https://orcid.org/0000-0003-1254-4817>
 Crystal L. Brogan  <https://orcid.org/0000-0002-6558-7653>
 Todd R. Hunter  <https://orcid.org/0000-0001-6492-0090>
 Anthony J. Remijan  <https://orcid.org/0000-0001-9479-9287>
 Geoffrey A. Blake  <https://orcid.org/0000-0003-0787-1610>
 Andrew M. Burkhardt  <https://orcid.org/0000-0003-0799-0927>
 Ewine F. van Dishoeck  <https://orcid.org/0000-0001-7591-1907>
 Robin T. Garrod  <https://orcid.org/0000-0001-7723-8955>
 Harold Linnartz  <https://orcid.org/0000-0002-8322-3538>
 Christopher N. Shingledecker  <https://orcid.org/0000-0002-5171-7568>
 Eric R. Willis  <https://orcid.org/0000-0002-7475-3908>

References

- Astropy Collaboration, Robitaille, T. P., Tollerud, E. J., et al. 2013, *A&A*, 558, A33
- Belloche, A., Garrod, R. T., Müller, H. S. P., & Menten, K. M. 2014, *Sci*, 345, 1584
- Benz, A. O., Bruderer, S., van Dishoeck, E. F., et al. 2010, *A&A*, 521, L35
- Bøgelund, E. G., McGuire, B. A., Ligterink, N. F. W., et al. 2018, *A&A*, 615, A88
- Brogan, C. L., Hunter, T. R., Cyganowski, C. J., et al. 2016, *ApJ*, 832, 1
- Brogan, C. L., Hunter, T. R., Cyganowski, C. J., et al. 2018, *ApJ*, submitted
- Carroll, P. B., Drouin, B. J., & Widicus Weaver, S. L. 2010, *ApJ*, 723, 845
- Ceccarelli, C., Bacmann, A., Boogert, A., et al. 2010, *A&A*, 521, L22
- Chibueze, J. O., Omodaka, T., Handa, T., et al. 2014, *ApJ*, 784, 114
- Comito, C., Schilke, P., Gerin, M., et al. 2003, *A&A*, 402, 635
- Crockett, N. R., Bergin, E. A., Neill, J. L., et al. 2014, *ApJ*, 787, 112
- de Graauw, T., Helmich, F. P., Phillips, T. G., et al. 2010, *A&A*, 518, L6
- De Luca, M., Gupta, H., Neufeld, D., et al. 2012, *ApJL*, 751, L37
- Emprechtinger, M., Lis, D. C., Rolffs, R., et al. 2013, *ApJ*, 765, 61
- Fayolle, E. C., Öberg, K. I., Jørgensen, J. K., et al. 2017, *NatAs*, 1, 703
- Fedoseev, G., Cuppen, H. M., Ioppolo, S., Lamberts, T., & Linnartz, H. 2015, *MNRAS*, 448, 1288
- Hollenbach, D., Elitzur, M., & McKee, C. F. 2013, *ApJ*, 773, 70
- Hunter, T. R., Brogan, C. L., MacLeod, G. C., et al. 2018, *ApJ*, 854, 170
- Jørgensen, J. K., Favre, C., Bisschop, S. E., et al. 2012, *ApJL*, 757, L4
- Lis, D. C., Pearson, J. C., Neufeld, D. A., et al. 2010, *A&A*, 521, L9
- MacLeod, G. C., Smits, D. P., Goedhart, S., et al. 2018, *MNRAS*, 478, 1077
- McGuire, B. A., Shingledecker, C. N., Willis, E. R., et al. 2017, *ApJL*, 851, L46
- Melnick, G. J., Ashby, M. L. N., Plume, R., et al. 2000, *ApJL*, 539, L87
- Melnick, G. J., Menten, K. M., Phillips, T. G., & Hunter, T. 1993, *ApJL*, 416, L37
- Messer, J. K., & De Lucia, F. C. 1984, *JMoSp*, 105, 139
- Müller, H. S. P., Schlöder, F., Stutzki, J., & Winnewisser, G. 2005, *JMoSt*, 742, 215
- Neill, J. L., Bergin, E. A., Lis, D. C., et al. 2014, *ApJ*, 789, 8
- Neill, J. L., Wang, S., Bergin, E. A., et al. 2013, *ApJ*, 770, 142
- Neufeld, D. A., Snell, R. L., Ashby, M. L. N., et al. 2000, *ApJL*, 539, L107
- Ossenkopf, V., Müller, H. S. P., Lis, D. C., et al. 2010, *A&A*, 518, L111
- Pilbratt, G. L., Riedinger, J. R., Passvogel, T., et al. 2010, *A&A*, 518, L1
- Reid, M. J., Menten, K. M., Brunthaler, A., et al. 2014, *ApJ*, 783, 130
- Requena-Torres, M. A., Martín-Pintado, J., Rodríguez-Franco, A., et al. 2006, *A&A*, 455, 971
- Russeil, D., Zavagno, A., Motte, F., et al. 2010, *A&A*, 515, A55
- San José-García, I., Mottram, J. C., van Dishoeck, E. F., et al. 2015, *A&A*, 585, A103
- Turner, B. E. 1991, *ApJS*, 76, 617
- van der Tak, F. F. S., Chavarría, L., Herpin, F., et al. 2013, *A&A*, 554, A83
- Zernicke, A., Schilke, P., Schmiedeke, A., et al. 2012, *A&A*, 546, A87